

1 **Assessing the ecological niche and invasion potential of the Asian giant hornet**

2

3 Gengping Zhu<sup>a,\*</sup>, Javier Gutierrez Illan<sup>a</sup>, Chris Looney<sup>b</sup>, David W. Crowder<sup>a</sup>

4 <sup>a</sup> Department of Entomology, Washington State University, Pullman, WA 99164, USA

5 <sup>b</sup> Washington State Department of Agriculture, Olympia, WA, 98501, USA

6 \* [gengping.zhu@wsu.edu](mailto:gengping.zhu@wsu.edu)

7

8 **Author Contributions**

9 All authors designed the study and wrote the manuscript, GZ conducted the analyses

10

11 **Competing Interest Statement:** None

12

13 **This file includes:**

14 Main Text

15 Figures 1 to 4

16

17 **Word Count:** 3484

18

19 **Reference Count:** 33

20

21 **Abstract**

22 The Asian giant hornet (*Vespa mandarinia*) is the world's largest hornet. It is native to East Asia,  
23 but was recently detected in British Columbia, Canada, and Washington State, USA. *Vespa*  
24 *mandarinia* are an invasion concern due to their potential to negatively affect honey bees and act  
25 as a human nuisance pest. Here, we assessed effects of bioclimatic variables on *V. mandarinia*  
26 and used ensemble forecasts to predict habitat suitability for this pest globally. We also simulated  
27 potential dispersal of *V. mandarinia* in western North America. We show that *V. mandarinia* are  
28 most likely to invade areas with warm to cool annual mean temperature but high precipitation,  
29 and could be particularly problematic in regions with these conditions and high levels of human  
30 activity. We identified regions with suitable habitat on all six continents except Antarctica. The  
31 realized niche of introduced populations in the USA and Canada was small compared to native  
32 populations, implying high potential for invasive spread into new regions. Dispersal simulations  
33 showed that without containment, *V. mandarinia* could rapidly spread into southern Washington  
34 and Oregon, USA and northward through British Columbia, Canada. Given its potential negative  
35 impacts, and the capacity for spread within northwestern North America and worldwide, strong  
36 mitigation efforts are needed to prevent further spread of *V. mandarinia*.

37

38 **Key words:** ecological niche model, climate suitability, human disturbance, ensemble forecast,  
39 pest management, dispersal

40

## 41 **Introduction**

42 The Asian giant hornet (*Vespa mandarinia* Smith) is the world's largest hornet and is native to  
43 temperate and sub-tropical Eastern Asia (Fig. 1A), where it is a predator of honey bees and other  
44 insects (Matsuura & Sakagami 1973; Archer 1995; McGlenaghan et al. 2019). Coordinated  
45 attacks by *V. mandarinia* on beehives involve pheromone marking to recruit other hornets,  
46 followed by rapid killing of worker bees until the hive is destroyed (McClenaghan et al. 2019).  
47 Japanese honey bees (*Apis cerana*) co-evolved with *V. mandarinia* and have defensive behaviors  
48 to counter these attacks, including recognizing and responding to marking pheromones and “bee  
49 ball” attacks on hornet workers (Sugahara et al. 2012; McGlenaghan et al. 2019). *Apis mellifera*,  
50 the European honey bee, however, has no co-evolutionary history with *V. mandarinia* and lacks  
51 effective defensive behaviors, making it highly susceptible to attack (McGlenaghan et al. 2019).

52 In September 2019, a nest of *V. mandarinia* was found on Vancouver Island in Canada, and  
53 two workers were found 90 km away in Washington State, USA, later that year (USDA 2019)  
54 (Fig. 1B). The introduction of Asian giant hornet into western North America is concerning  
55 because of the vulnerability of *A. mellifera*, which is widely used for crop pollination, to hornet  
56 attacks. Predation by *V. mandarinia* on *A. mellifera* in Asia causes major losses (McGlenaghan et  
57 al. 2019). *Vespa mandarinia* is also medically significant, and can deliver painful stings and large  
58 doses of cytolytic venom. Multiple stings can be fatal even in non-allergic individuals, although  
59 recent mortality rates are much lower than the historic reports of more than 30 yearly deaths in  
60 Japan (Yanagawa et al. 2007). Currently, *V. mandarinia* is listed as a quarantine pest of the  
61 United States and efforts are underway to prevent establishment and spread (USDA 2019).

62 Invasions from species such as *V. mandarinia* are governed by arrival, establishment, and  
63 spread (Liebhold & Tobin 2008). Ecological niche models, which involve model calibration  
64 using climate variables in native ranges, followed by extrapolation to introduced areas, are often  
65 used to assess habitat suitability for invasive species (Liebhold & Tobin 2008; Peterson et al.  
66 2013). Invasions can be particularly problematic in regions with high human activity, which can  
67 also facilitate invasions through transport of introduced species. To assess spread of invasive  
68 species, models can also simulate processes (Liebhold & Tobin 2008; Engler et al. 2012). Models  
69 thus guide efforts to prevent establishment and spread, which are cost-effective early in invasions  
70 (Liebhold & Tobin 2008).

71 It is not yet clear if *V. mandarinia* is established in North America, and federal and local  
72 agencies are implementing trapping and monitoring programs to identify areas of introduction  
73 and prevent establishment and spread (USDA 2019). However, several factors that could guide  
74 mitigation efforts remain unknown, including the potential habitat suitability for *V. mandarinia*.  
75 Moreover, the potential rate of population dispersal into new areas is poorly understood. In  
76 Europe, an invasion by the congener *V. velutina* has expanded via natural and human-assisted  
77 dispersal from 19 to nearly 80 km per year (Bertolino et al. 2016; Robinet et al. 2017). Here, we  
78 assess these questions by modeling responses of *V. mandarinia* to bioclimatic variables in the  
79 native range and extrapolating to introduced ranges. We also used dispersal simulations to  
80 estimate potential rates of spread throughout western North America. These complementary  
81 approaches can guide efforts to prevent the establishment and spread of this invasive species.

82

## 83 **Material and Methods**

### 84 *Environmental factors affecting occurrence of V. mandarinia*

85 We first assessed relationships between occurrence of *V. mandarinia* and environmental  
86 factors. Occurrence data were attained with the “spocc” package in R (R Core Team 2020) from  
87 the Global Biodiversity Information Facility, Biodiversity Information Serving Our Nation,  
88 Integrated Digitized Biocollections, and iNaturalist (Scott et al. 2017) (Fig. 1). Additional data  
89 were collected from published studies (Archer 1995; Lee 2010). Occurrence records located  
90 within oceans or without geographic coordinates were removed. 422 unique records from *V.*  
91 *mandarinia*’s native range in Asia (Japan, South Korea, Taiwan) were obtained (Fig. 1A). Of  
92 these, 200 were filtered out by enforcing a distance of 10 km between records (Fig. 1A); we used  
93 this filtering process because ecological niche models are sensitive to sample bias (Warren &  
94 Seifert 2011). Our assembled 222 records from east Asia are consistent with published records  
95 (Archer 1995; Lee 2010), suggesting we effectively captured the distribution of *V. mandarina*.

96 Vespine wasps have high endothermic capacity and thermoregulatory efficiency, and can  
97 survive broad temperature ranges (Käfer et al. 2012). To determine climate factors that constrain  
98 *V. mandarinia*, we obtained 7 Worldclim variables (Fick & Hijmans 2017): (i) annual mean  
99 temperature, (ii) mean diurnal range, (iii) max temperature of warmest month, (iv) minimum  
100 temperature of coldest month, (v) annual precipitation, (vi) precipitation of wettest and (viii)  
101 driest months (Bio14); we also considered annual mean radiation (Fig. S1A). Although some of  
102 these variables were correlated (Fig. S1B), highly correlated variables have little impact on  
103 ecological niche models that account for redundant variables (Feng et al. 2019).

104           After selecting variables, we used generalized linear models (GLM) with Bernoulli errors  
105 to model the probability of occurrence of *V. mandarinia* as a function of each bioclimatic factor.  
106 This approach was used to minimize the chances of overfitting models, and Hosmer Lemeshow  
107 goodness of fit test were used to evaluate GLM model performance (Hosmer et al. 1989). Rather  
108 than plotting a single partial response curve (i.e., fitting response curves for specific predictors  
109 while keeping the other predictors at their mean value), we adopted inflated response curves to  
110 explore species-environment relationships along the entire gradient while keeping the other  
111 predictors at their mean, minimum, median, maximum, and quartile values (Zurell et al. 2012).

112

### 113 ***Realized niche modeling of native and introduced populations***

114           After assessing environmental factors affecting *V. mandarinia* occurrence, we next assessed  
115 realized niches occupied by native and introduced populations. Given that only 4 occurrence  
116 points exist in the introduced range of western North America, two of which are within 10 km,  
117 we could not use a strict test of whether realized niches shifted during the introduction of *V.*  
118 *mandarinia* (i.e., niche equivalency and similarity test; Warren et al. 2010). Rather, we used  
119 minimum ellipsoid volumes to display and compare the two realized niches; this technique  
120 provides a clear vision of niche breadth for two populations and their relative positions in  
121 reduced dimensions (Qiao et al. 2016). We generated three environmental dimensions that  
122 summarized 90% of overall variations in the 8 global bioclimatic dimensions using principle  
123 component analysis in NicheA version 3.0 (Qiao et al. 2016).

124

125 ***Ecological niche modeling***

126 We used classical niche models to assess worldwide habitat suitability for potential spread  
127 of *V. mandarinia* (Peterson et al. 2013). Given that uncertainty exists with any individual model,  
128 we used an ensemble approach that averaged predictions of five algorithms: (i) generalized  
129 additive models, (ii) general boosted models, (iii) generalized linear models; (iv) random forests,  
130 and (v) maximum entropy models. Such ensemble models have been proposed as a consensus  
131 approach to more effectively estimate climate suitability, achieve a higher predictive capacity,  
132 and reduce uncertainty (Araújo & New 2007; Thuiller et al 2009; Zhu & Peterson 2017). To  
133 build models, 50% of observed records were used for model training and 50% for validation  
134 (Tsoar et al. 2007). We used a “random” method in *biomod2* to select 10,000 pseudo-absence  
135 records from “accessible” areas of *V. mandarinia* in Asia, which were delimited by buffering  
136 minimum convex polygons of observed points at 400 km (Owen et al. 2013). This selection of  
137 pseudo-absence records improves ecological niche model performance (Phillips & Dudík 2008).

138 For evaluation of models, we used Area Under the Curve (AUC) of Receiver Operating  
139 Characteristic (ROC) plots as a measure of model fit (Jiménez-Valverde et al. 2012). AUC has  
140 been criticized in niche model literature, and inference upon its values should be taken cautiously  
141 as we didn't have reliable absence data (Leroy et al. 2012). However, here we simply tested  
142 niche model discriminability in native areas and not introduced areas. Final niche models were  
143 fitted using overall trimmed occurrence points for combination with footprint and displaying.

144 Habitat modification and disruption has been linked to invasiveness in some Vespidae, and  
145 invasions could be particularly problematic in regions with high human activity (Beggs et al.

146 2011, Robinet et al. 2017). In its native range, *V. mandarinia* is able to colonize green areas in  
147 cities, although at lower abundance than other vespine wasps (Choi et al. 2012). Human-assisted  
148 movement has affected expansion of *V. velutina* in Europe, and may also affect *V. mandarinia*  
149 (Robinet et al 2007). Models that combine climate suitability with measures of human activity  
150 may provide more accurate estimates of site vulnerability to colonization, particularly arrival and  
151 establishment processes (Liebhold & Tobin 2008). We measured human footprint as an indicator  
152 of human-mediated disturbances, a metric that combines population pressure and human  
153 infrastructure. We combined human footprint with climate suitability using a bivariate mapping  
154 approach (Fig. 2). All variables selected for analyses were used at a resolution of 5 arcmin.

155

### 156 ***Dispersal simulation***

157 *Vespa mandarinia* is a social insect that forms colonies with one queen and many workers,  
158 and population dispersal is mediated by the spread of queens. Workers typically fly 1 to 2 km  
159 from their nest when foraging, although they can forage up to 8 km (Matsuura & Sakagami  
160 1973). Data on queen dispersal appears to be unknown, but *V. mandarinia* queens are likely to  
161 have flight capacity greater than workers. Flight mill simulations with the congener *V. velutina*  
162 suggest that queens can fly 18 km in a single day (Robinet et al 2017), although flight distance  
163 under field conditions is likely to be smaller.

164 To simulate potential spread of *V. mandarinia* based on these dispersal capacities and  
165 occurrence points in western North America, we used the “MigClim” package (Engler et al.  
166 2012). This approach simulates species expansion using a species’ occurrence as well as habitat



167 suitability and different dispersal scenarios. Short-distance dispersal considers innate dispersal of  
168 a species to move through diffusion-based processes, whereas long-distance dispersal considers  
169 passive dispersal over long distance, such as dispersal by hitchhiking on human activity (Engler  
170 et al. 2012). MigClim uses a dispersal step as a basic time unit to simulate the dispersal, with  
171 dispersal steps often equal to one year since most organism dispersal occurs yearly or can be  
172 modeled as such, particularly for social insects where queens form colonies only once a year  
173 (Engler et al. 2012). We ran a simulation with a total of 20 dispersal steps for *V. mandarinia*.

174 In our simulations, we created combined suitability using climate suitability from ensemble  
175 models and human footprint. We then chose 3 different dispersal scenarios for simulations: (i)  
176 short-distance dispersal only, (ii) long-distance dispersal only, and (iii) both short- and  
177 long-distance dispersal. These three scenarios seek to capture both biological and  
178 human-mediated dispersal potential of *V. mandarinia*, as MigClim does not account for  
179 population demography (Engler et al. 2012). Simulations of short-distance dispersal were based  
180 on physical barriers and the dispersal kernel, which is the dispersal probability as a function of  
181 distance, whereas long-distance dispersal simulations depend on frequency of movement and  
182 distance range. MigClim uses a dispersal step as a basic time unit to simulate the dispersal, with  
183 dispersal steps often be equal to one year since most organism dispersal occurs yearly or can be  
184 modeled as such, particularly for social insects where queens form colonies only once a year  
185 (Engler et al. 2012).

186 We ran simulations with 20 dispersal steps. In MigClim, the dispersal kernel is the dispersal  
187 probability as a function of distance ( $P_{disp}$ ) and the propagule production potential ( $P_{prop}$ ). Our

188 raster data had a resolution of 5 arcmin ( $\approx 5.5$  km); we defined short-distance dispersal as less  
189 than 6 pixels ( $\sim 33$ km). Dispersal more than 6 pixels was considered long-distance dispersal,  
190 which had a maximum 20 pixels ( $\sim 110$ km). We used a dispersal kernel of 1.0, 0.4, 0.16, 0.06,  
191 and 0.03 pixel for short-distance dispersal, which is an average of 10 km/dispersal step, with a  
192 maximum of 33 km. We set  $P_{prop}$  as 1 since *V. mandarinia* is a social insect and we assumed that  
193 the probability of a source cell to produce propagules is 100%. We assumed there were no  
194 barriers to either short- or long-distance dispersal.

195

## 196 **Results and Discussion**

197 Generalized linear models showed no significant differences between models fit to the 8  
198 environmental variables and observed data ( $\chi^2 = 8.2$ ,  $df = 8$ ,  $P = 0.41$ ). We show *V. mandarinia* is  
199 most likely to occur in regions with low to warm annual mean temperatures and high annual  
200 precipitation (Fig. 2). However, our models show that they can tolerate broad temperature ranges  
201 (Fig. 2, S3), and that they are not particularly sensitive to radiation and extremes of precipitation  
202 (Fig. S3). The most suitable habitats are predicted to be in regions with maximum temperature of  
203 39 °C in the warmest month (Fig. S3). Our results thus support the existence of a thermal  
204 threshold beyond which *V. mandarina* would be unable to establish, and this could be crucial for  
205 management and policy making in case of a prolonged invasion of the hornet in North America.

206 The minimum ellipsoid volumes show that the realized niche of introduced individuals in  
207 western North America were nested within the realized niche of native populations (Fig. 3). As  
208 the introduced locations represent a small fraction of the realized niche occupied by native

209 populations, there is widespread potential for the introduced range to expand without mitigation  
210 (Fig. 3). However, the contrasting volume sizes occupied by native and introduced populations  
211 may simply be due to the limited number of occurrences outside of the native range (4 points)  
212 rather than any reduction in the niche space available to introduced populations.

213 Our ecological niche models showed excellent performance in discriminability evaluations  
214 (generalized additive model [GAM]: AUC = 0.89; general boosted model [GBM]: AUC = 0.93;  
215 generalized linear model [GLM]: AUC = 0.91; Maxent: AUC = 0.93; Random Forest [RF]: AUC  
216 = 0.91). However, the five niche models had variability in habitat suitability across the globe  
217 (Fig. S4), and the ensemble model (Fig. 2) had better discriminability and outperformed these  
218 individual models (AUC = 0.94). Outside of the native area, our ensemble models captured  
219 detection points in North America as occurring in regions with highly suitable habitat (Fig. 2).

220 The ensemble models suggested that suitable habitat for *V. mandarinia* exists along much of  
221 the coastline of western North America as most of the eastern USA and adjacent parts of Canada,  
222 much of Europe, northwestern and southeastern South America, central Africa, eastern Australia,  
223 and most parts of New Zealand. Each of these regions is also associated with high human activity,  
224 although we did identify suitable climatic areas with low human activity (e.g., central South  
225 America, Fig. 2). Yet, given that many suitable regions were identified by the ensemble model  
226 that had both high climatic suitability and high human activity, it is likely that human activity  
227 could facilitate future invasions of *V. mandarinia*. The model predicts that much of the interior of  
228 North America is unsuitable habitat, likely due to inhospitable temperatures and low  
229 precipitation. This includes the eastern portions of British Columbia and the Pacific Northwest

230 states, and the Central Valley of California, all of which have extensive agricultural production  
231 (e.g. tree fruit and tree nuts) that relies almost exclusively on *A. mellifera* pollination.

232 Our simulations of *V. mandarinia* dispersal in western North America showed high potential  
233 for spread within western North America (Fig. 4). When considering short-distance dispersal,  
234 mediated by hornets flying an average of 10 km/yr and a maximum of 33 km/yr, populations of *V.*  
235 *mandarinia* could rapidly spread along the western coast of North America, reaching Oregon in  
236 20 yr. Northward expansion into Canada would likely be limited to the southern coast of British  
237 Columbia (Fig. 4). When we accounted for long-distance human-mediated dispersal, the  
238 expansion of *V. mandarinia* extended dramatically toward the north along coastal areas of British  
239 Columbia, and showed a faster rate of expansion into southern Washington State and into Oregon,  
240 USA (Fig. 4). This suggests dispersal throughout the western USA could occur within 20 or less  
241 yr even without human-mediated transport or new introduction events.

242 Ecological impacts are difficult to predict for vespids (Beggs et al. 2011). While many  
243 transplanted Vespidae appear to have only minor impacts, others are known to displace  
244 congeners through multiple, idiosyncratic mechanisms (Beggs et al 2011). There are no other  
245 *Vespa*, native or introduced, in the region of North America where *V. mandarinia* has been  
246 detected, and no native *Vespa* where suitable habitat is predicted by this model. However, Asian  
247 giant hornets are known to prey on social Hymenoptera other than bees (Matsuura 1984), and  
248 thus could affect populations of several vespid genera in the Pacific Northwest. *Vespa*  
249 *mandarinia* also preys upon many other insects, with chafer beetles comprising a large part of its  
250 diet in parts of Japan (Matsuura 1984). It is unknown how it might impact native insects if it

251 becomes established, but the habitat suitability predicted here indicates that negative effects  
252 could be distributed over a fairly expansive area.

253 We also anticipate considerable impacts on beekeepers. Established populations of *V.*  
254 *mandarinia* would likely prey on readily-available hives late in the season, weakening any that  
255 aren't killed outright. In Europe, the congener *V. velutina* has reportedly caused losses ranging  
256 from 18 to 80% of domestic hives, depending on the region (Laurino et al. 2020). The results  
257 presented here suggest that large expanses of the Pacific Coast in North America could become  
258 challenging for beekeeping operations, especially during the late summer and fall when attacks  
259 are greatest. Unchecked, this species of hornet could cause major disruption in the western US  
260 and Canada, possibly forcing beekeepers to invest in extensive hornet management or relocate  
261 parts of their operations to areas of unsuitable *V. mandarinia* habitat.

262

### 263 **Acknowledgement**

264 We thank D. Zurell, R. Engler, and E. Ugene for help developing ecological models. The  
265 work was funded by USDA Hatch Project 1014754.

266 **References**

- 267 Araújo MB, New M (2007) Ensemble forecasting of species distributions. *Trends in Ecol. Evol.*  
268 22, 42–47.
- 269 Archer ME (1995) Taxonomy, distribution and nesting biology of the *Vespa mandarinia* group  
270 (HYM. Vespinae). *Entomol. Mon. Mag.* 131, 47–53.
- 271 Beggs JR et al. (2011) Ecological effects and management of invasive alien Vespidae. *Biocontrol*  
272 56: 505-526.
- 273 Bertolino S, Liroy S, Laurino D, Manino A, Porporato M (2016) Spread of the invasive yellow-  
274 legged hornet *Vespa velutina* (Hymenoptera: Vespidae) in Italy. *Appl. Entomol. Zool.*, 51,  
275 589–597.
- 276 Choi MB, Kim JK, Loo JW (2012) Increase trend of social Hymenoptera (wasps and honeybees)  
277 in urban areas, inferred from moving-out case by 119 rescue services in Seoul of South  
278 Korea. *Entomol. Res.* 42, 308–319.
- 279 Engler R, Hordijk W, Guisan A (2012) The MIGCLIM R package – seamless integration of  
280 dispersal constraints into projections of species distribution models. *Ecography* 35,  
281 872–878.
- 282 Feng X, Park DS, Liang Y, Pandey R, Papeş M (2019) Collinearity in ecological niche modeling:  
283 Confusions and challenges. *Ecol. Evol.* 9, 10365–10376.
- 284 Fick SE, Hijmans RJ (2017) WorldClim 2: new 1km spatial resolution climate surfaces for global  
285 land areas. *Int. J. Clim.* 37, 4302-4315.

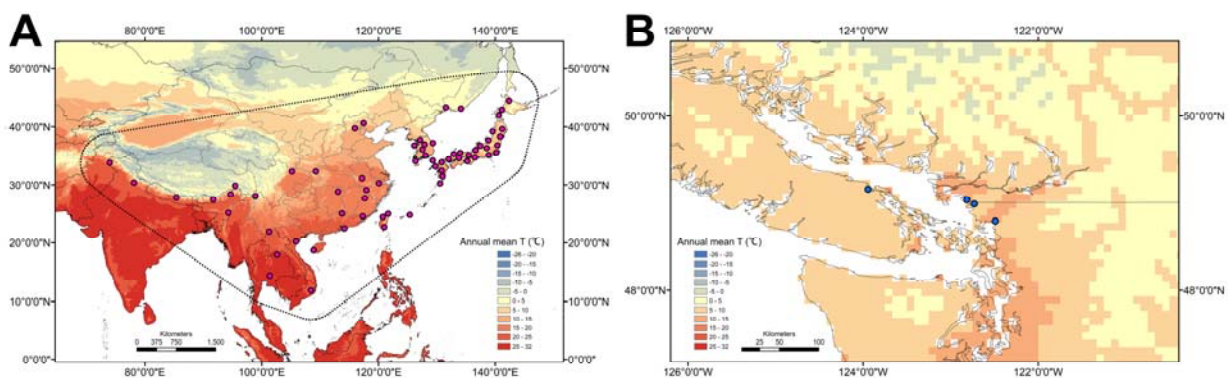
- 286 Hosmer DW, Jovanovic B, Lemeshow S (1989) Best subsets logistic regression. *Biometrics* 45,  
287 1265–1270.
- 288 Käfer H, Kovac H, Stabentheiner A (2012) Resting metabolism and critical thermal maxima of  
289 vespine wasps (*Vespula* sp.) *J. Insect Phys.* 58, 679–689.
- 290 Laurino D, Lioy S, Carisio L, Manino A, Porporato M (2020) *Vespa velutina*: An alien driver of  
291 honey bee colony loss. *Diversity* 12, 5.
- 292 Lee JX (2010) Notes on *Vespa analis* and *Vespa mandarinia* (Hymenoptera, Vespidae) in Hong  
293 Kong, and a key to all *Vespa* species known from the SAR. *Hong Kong Entomol. Bull.* 2,  
294 31–36.
- 295 Leroy B et al. (2018) Without quality presence–absence data, discrimination metrics such as TSS  
296 can be misleading measures of model performance. *J. Biogeog.* 45, 1994–2002.
- 297 Liebhold AM, Tobin PC (2008) Population ecology of insect invasions and their management.  
298 *Annu. Rev. Entomol.* 53, 387–408.
- 299 Matsuura M (1984) Comparative biology of the five Japanese species of the genus *Vespa*  
300 (Hymenoptera, Vespidae). *Bull Fac. Agric. Mie Univ.* 69, 1–131.
- 301 Matsuura M, Sakagami SF (1973) A bionomic sketch of the giant hornet, *Vespa mandarinia*, a  
302 serious pest for Japanese apiculture. *J. Fac. Sci Hokkaido Univ. (Zoology)* 19, 125–162.
- 303 McClenaghan B et al. (2019) Behavioral responses of honey bees, *Apis cerana* and *Apis*  
304 *mellifera*, to *Vespa mandarinia* marking and alarm pheromones. *J. Apic. Res.* 58, 141–148.
- 305 Owens HL et al. (2013) Constraints on interpretation of ecological niche models by limited  
306 environmental ranges on calibration areas. *Ecol. Model.* 263, 10–18.

- 307 Peterson AT et al. (2011) *Ecological Niches and Geographic Distributions: A Modeling*  
308 *Perspective*. Princeton University Press, Princeton, USA.
- 309 Phillips SJ, Dudík M (2008) Modeling of species distributions with Maxent: new extensions and  
310 a comprehensive evaluation. *Ecography* 31, 161–175.
- 311 Qiao H, Peterson AT, Campbell LP, Soberon J, Ji L, Escobar LE (2016) NicheA: creating virtual  
312 species and ecological niches in multivariate environmental scenarios. *Ecography* 39,  
313 805-813.
- 314 R Core Team (2020) R: a language and environment for statistical computing (v. 4.0.0). R  
315 Foundation for Statistical Computing, Vienna, Austria.
- 316 Robinet C, Suppo C, Darrouzet E (2017) Rapid spread of the invasive yellow-legged hornet in  
317 France: The role of human-mediated dispersal and the effects of control measures. *J. Appl.*  
318 *Ecol.* 54, 205–215.
- 319 Scott A, Ram K, Hart T, Chamberlain MS (2017) spocc: interface to species occurrence data  
320 sources, R package version 0.4.0. Available: <http://CRAN.R-project.org/package=spocc>.
- 321 Sugahara M, Nishimura Y, Sakamoto F (2012) Differences in heat sensitivity between Japanese  
322 honeybees and hornets under high carbon dioxide and humidity conditions inside bee balls.  
323 *Zool. Sci.* 29, 30–36.
- 324 Thuiller W, Lafourcade B, Engler R, Araújo MB (2009) BIOMOD—a platform for ensemble  
325 forecasting of species distributions. *Ecography* 32, 369–373.
- 326 Tsoar, A., Allouche, O., Steinitz, O., Rotem, D. and Kadmon, R., 2007. A comparative evaluation  
327 of presence-only methods for modelling species distribution. *Div. Dist.* 13, 397-405.



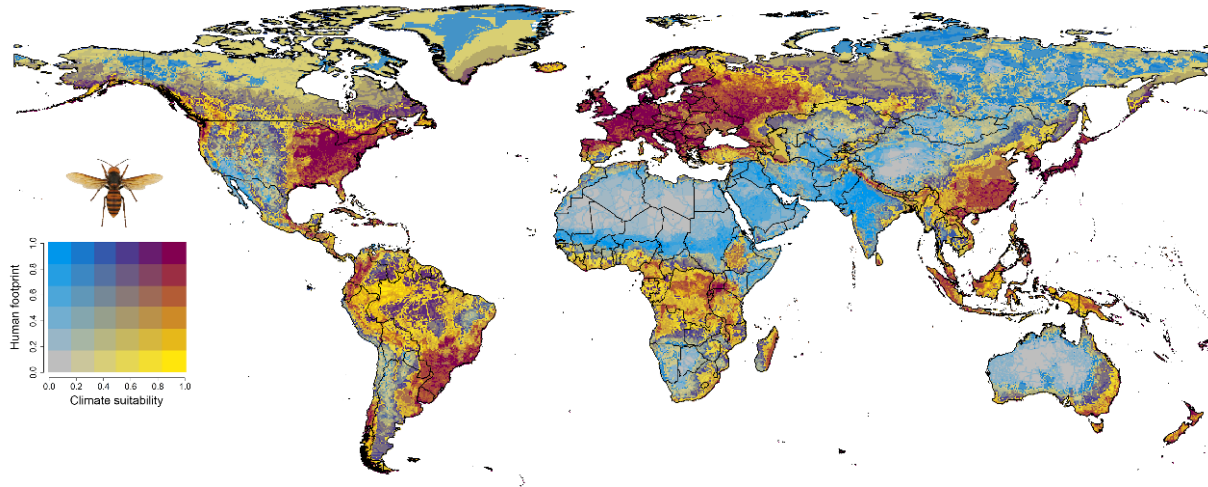
- 328 USDA (2019) New pest response guidelines for Asian giant hornet (*Vespa mandarinia*). United  
329 States Department of Agriculture, Animal and Plant Health Inspection Service, Plant  
330 Protection and Quarantine, Riverdale Park, MD, USA.
- 331 Warren DL, Glor RE, Turelli M (2010) ENMTools: a toolbox for comparative studies of  
332 environmental niche models. *Ecography* 33: 607–611.
- 333 Warren DL, Seifert SN (2011) Ecological niche modeling in Maxent: the importance of model  
334 complexity and the performance of model selection criteria. *Ecol. Appl.* 21, 335–342.
- 335 Yanagawa Y, Morita K, Sugiura T, Okada Y (2007) Cutaneous hemorrhage or necrosis findings  
336 after *Vespa mandarinia* (wasp) stings may predict the occurrence of multiple organ injury:  
337 A case report and review of literature. *Clin. Toxicol.* 45, 803–807.
- 338 Zhu GP, Peterson AT (2017) Do consensus models outperform individual models? Transferability  
339 evaluations of diverse modeling approaches for an invasive moth. *Biol. Invasions* 19,  
340 2519–2532.
- 341 Zurell D, Elith J, Schroeder B (2012) Predicting to new environments: tools for visualizing  
342 model behavior and impacts on mapped distributions. *Div. Dist.* 18, 628–634.

343 **Figure 1.** Present distribution of Asian giant hornet in (A) native and (B) introduced regions. In  
344 (A) points denote trimmed records used to fit models.  
345



346

347 **Figure 2.** Ensemble forecast of potential invasion of *Vespa mandarinia*. Increasing intensities of  
348 yellow represent increasing climate suitability, and increasing blue represent increasing  
349 establishment potential due to human activity, where increasing red mean increasing potential  
350 invasion due to high climate suitability and human activity. Scores of bivariate maps are divided  
351 into 6 equal quantiles in the data ranges of climate suitability and human footprint respectively.  
352

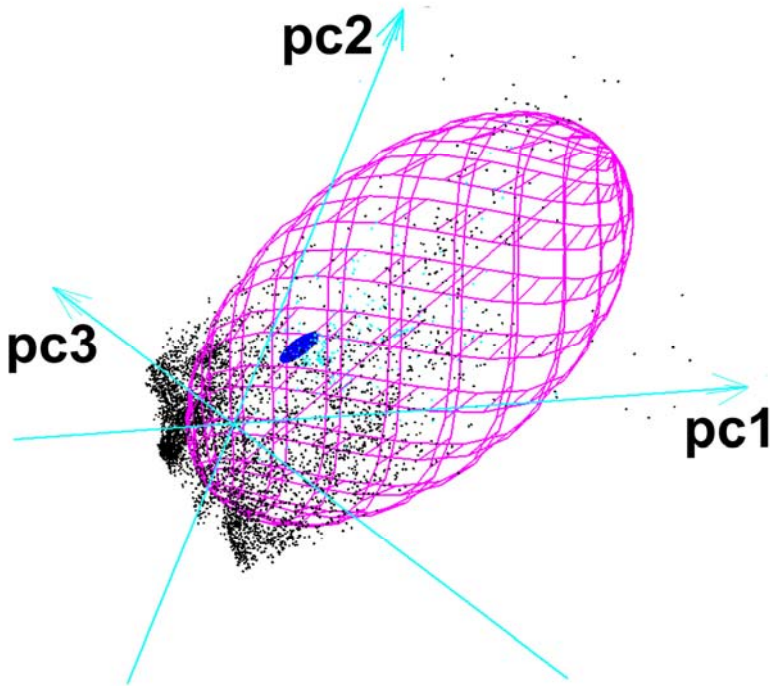


353

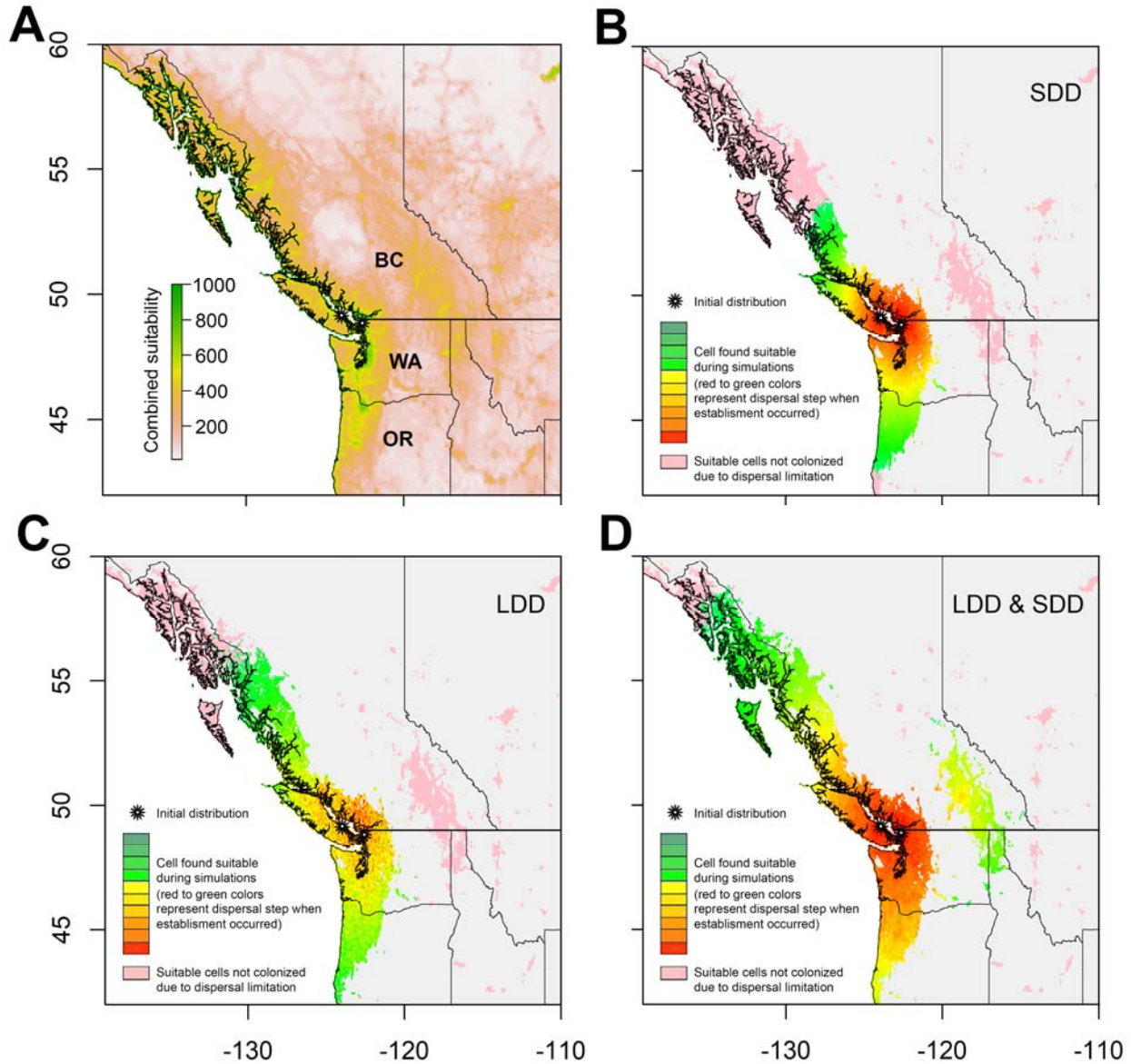
354

355

356 **Figure 3.** Realized niche occupied by native and introduced populations shown as minimum  
357 ellipsoid volumes. The pink volume represents the native niche, the blue volume represents the  
358 introduced niche, and points denote environmental conditions across the globe. The three PCA  
359 axes were estimated in NicheA and captured 90% of the variation in the 8 bioclimatic variables.  
360  
361  
362



363 **Figure 4.** Combined suitability (A) and estimated expansion (B-D) of *Vespa mandarinia* over 20  
364 yr in western North America under three dispersal scenarios: (B) short dispersal distance only  
365 (SSD), (C) long dispersal distance only (LDD) and (D) combined (LDD & SDD) scenarios. Each  
366 color represents two dispersal steps (total 20 dispersal steps) in dispersal simulations.



367